

***IN VITRO* EFFECT OF PAROMOMYCIN CONJUGATED NANOCHITOSAN ON *E. HISTOLYTICA* TROPHOZOITES**

^{1*}Hajar Falih Hishan Aldali, ²Shatha Khudiar Abbas, ³Ahmed Naji Abd

^{1,2,3}Department of Biology, College of Science, Almustansiriyah University, Baghdad, Iraq, *Corresponding author

Abstract

Entamoeba histolytica is a parasite of the intestinal tract that infects humans and causes inflammation of the intestinal tissues, and the infection may reach other sites, such as the liver. This study aimed to measure the effect of paromycin conjugated nano-chitosan in inhibiting the trophozoites of the parasite *in vitro*. Nanochitosan was prepared and the antibiotic was loaded using ultrasound and the FTIR spectroscopy was used to describe the materials prepared. *Entamoeba histolytica* trophozoites were grown on She medium, then the effect of the prepared material was studied using the MTT method. The results of the current study indicate the inhibitory effect of paromycin conjugated nanochitosan in inhibiting the growth of the trophozoites compared to nanochitosan and paromomycin as the IC₅₀s were 44.41, 106.5 and 27.47 µg/mL after 24h. for nanochitosan, paromomycin and paromomycin conjugated nanochitosan respectively.

Key words: Chitosan, *E. histolytica*, Nanomaterials, paromomycin, MTT.

Introduction

Protozoan parasites can infect the human digestive system and cause significant infections in addition to bacterial and viral pathogens (Hemphill *et al.*, 2019) *Entamoeba histolytica*, a major cause of intestinal amebiasis and amoebic liver abscess, is primarily found in the human gastrointestinal system which account for 100,000 fatalities annually around the world, *E. histolytica* enters host tissue by adhesion, contact-dependent lysis, and phagocytosis and this causes an initial inflammatory response (Flores-Huerta *et al.*, 2024). In *E. histolytica*, stage interconversion between the trophozoite and cyst stages is crucial for disease transmission and pathophysiology (Haque *et al.*, 2006) *E. histolytica*'s infectious cycle starts when the cyst, a non-dividing, quadrinucleate form that has a chitin-containing cell wall that protects it from the environment, is consumed. The proliferative trophozoite form is created in the small intestine by the cyst's excystation upon ingestion. Trophozoites adhere to the mucous layer of the colon to start a colony. When the intestinal epithelial cells are attacked by trophozoites through the breach in the mucus layer, disease ensues. Some trophozoites encyst for reasons that are unclear, which enables them to be expelled in the feces and infect new hosts (Ehrenkaufer *et al.*, 2007). The majority of patients have stomach pain, soreness, and diarrhea. Other symptoms of the infection include dysentery, acute necrotizing colitis, toxic megacolon, chronic non-dysenteric colitis, ameboma, and perianal ulceration (Hamad, 2021; Houpt *et al.*, 2016). Despite having unfavorable side effects (nausea, neurotoxicity, headache, and other unpleasant symptoms), metronidazole is the first treatment of choice for invasive amebiasis because of its wide lethal action against protozoa and



the majority of anaerobic bacteria (Azad *et al.*, 2023). However, the demand for innovative drugs has arisen due to adverse effects and resistance. Because of their reduced size, biocompatibility, and efficiency in penetrating tissues, nanoparticles have drawn attention. These substances are a viable substitute for metronidazole since they have different targets and modes of action (Zahra'a *et al.*, 2017). Nanomaterials have been extensively used in the domains of biomedicine and bioengineering, ranging from diagnostics to treatments. (Gupta *et al.*, 2024). Because of their vast surface area, chitosan nanoparticles are preferred because they have a high and effective adsorption capacity for the pollutant in suspension (Sivakami *et al.*, 2013) their positive charge of the chitosan amine groups effectively forms complexes with conjugate compounds and anionic polymers, enabling high target selectivity and immune activity. Moreover, chitosan's mucoadhesive qualities enable specific site absorption of chitosan nanoparticles. Because of this, chitosan nanoparticles (NPs) are often employed in pharmaceuticals and medicine to transport drugs, DNA, and vaccinations. Important steps in the delivery process include the safe encapsulation of the target molecule by NPs, its transport (with enzyme protection), and its appropriate release at the target location. NPs' dimensions, stability, binding affinities, and absorption increase (Lee *et al.*, 2023).

MATERIALS AND METHODS

Chitosan powder provided by Avonchem from the United Kingdom (U.K.) was used to prepare Nano chitosan by dissolving 1g of chitosan in 100 mL of deionized distilled water and heating to a temperature of 51 for 60 minutes after the samples were transferred to a sonicator for 30 minutes; Paromomycin (Humatin) capsules manufactured by (Pfizer Pharma PFE GmbH 250 mg, Germany) were diluted in Distilled water (1gm/ 100ml) then put in the ultrasonic bath for 30 minutes, The solution of chitosan nanoparticles was added to Paromomycin solution. It was then incubated in an ultrasonic bath for 15 min.

Five concentrations (200, 100, 50, 25 and 12.5) µg/mL were prepared for nanochitosan, paromomycin and paromomycin conjugated nanochitosan

Parasite Collection

Parasites were collected from stool samples of patients with diarrhoea who visited Emam Alli (A) hospital in Iraq from June to July 2022. The direct saline mount and Lugol's iodine wet mount for each stool sample were used to diagnose *E. histolytica* trophozoites and cysts microscopically (40X) (Jassim, 2014).

SHE-medium

The SHE media was prepared according to Ali *et al.*, (2009). then the parasite trophozoites the amount of 0.5 mg of positive stool sample contain (5-6) trophozoites was cultured on the SHE-medium.

MTT method

The MTT (3-[4,5-dimethylthiazol-2-yl]-2,5-diphenyl tetrazolium bromide) assay was done according to Van Meerloo *et al.*, (2011).

Fourier Transform Infrared Spectroscopy (FTIR):

To determine the functional groups and qualitative development of chitosan nanoparticles, the FTIR spectra of chitosan nanomaterials, paromomycin, and paromomycin-loaded chitosan nanomaterials were examined in the BPC facility in Baghdad. The intensity versus wave number of the Fourier transformed infrared spectroscopy (FT-IR) spectra, which were obtained between 400 and 4000 cm^{-1} , are displayed.

Statistical analysis

The data of the present study were expressed as mean value \pm SD and the differences between the groups were statistically analyzed by ANOVA. A P value ≥ 0.0001 was regarded as statistically significant.

Results and discussion

FTIR Measurements

FTIR spectroscopy serves as a valuable tool for discerning variations in the spectral bands of both organic and inorganic compounds within a given sample. It relies on the analysis of infrared absorption frequencies spanning the range of 400–4000 cm^{-1} . Through this method, we can identify molecular groups present in a sample, discover interaction bands between components in blended substances, and determine any alterations in these bands. Figure (1) presents the FTIR curve for a pure chitosan sample, which exhibits the following characteristic peaks:

The peak at 3422.69 cm^{-1} corresponds to OH stretching vibrations. The peak at 2871.30 cm^{-1} is associated with the C-H stretching aliphatic vibrations in the $-\text{CH}_2$ groups. Amide frequencies are represented by N-H bond stretching (amide I) at 1635.62 cm^{-1} and N-H straining vibrations of $-\text{NH}_2$ groups at 1539.22 cm^{-1} . A peak at 1375.39 cm^{-1} signifies the symmetric deformation of C-H in the $-\text{CH}_3$ group. The peak at 1325.12 cm^{-1} is attributed to the vibration modes of amide III. Stretching vibrations at 1063.48 cm^{-1} reveal the C-O stretching vibration of alcohol groups. It is worth noting that these FTIR bands have been observed by various authors in similar studies (El-araby, 2022; Rodrigues *et al.*, 2020 and Varma and Vasudevan, 2020).

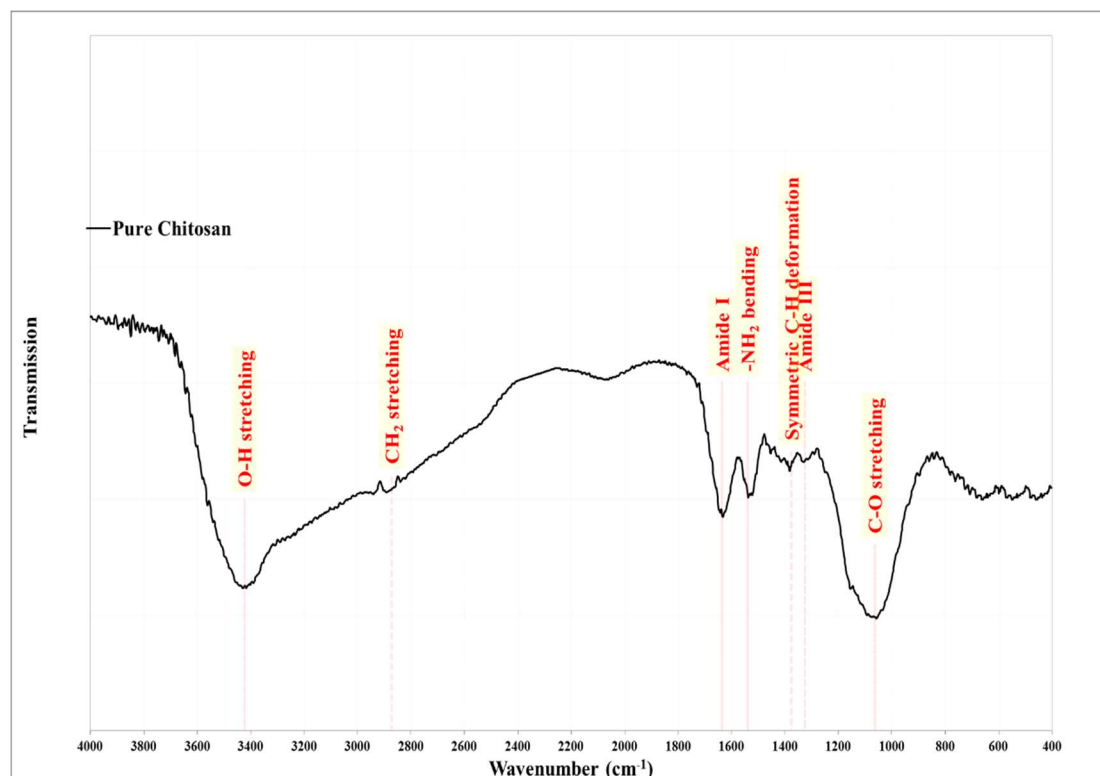


Figure 1: FTIR spectrum of chitosan

In Figure (2), the FTIR spectrum for pure Paromomycin is presented, revealing distinct characteristic peaks its molecular structure. These peaks and their corresponding assignments are as follows:

The peak at 3426.14 cm^{-1} is attributed to OH stretching vibrations. The peaks at 2922.93 and 2885.02 cm^{-1} are associated with the C-H stretching vibrations in the $-\text{CH}_2$ groups. N-H stretching bond is observed at 1627.00 cm^{-1} , and N-H straining vibrations of $-\text{NH}_2$ groups are noted at 1528.77 cm^{-1} . At 1077.26 cm^{-1} , the peak indicating the C-O stretching vibration. The band at 610.24 cm^{-1} is attributed to C-H vibrations. It's worth mentioning that these findings are consistent with the results reported in reference (Khan and Kumar, 2011 and Afzal *et al.*, 2019).

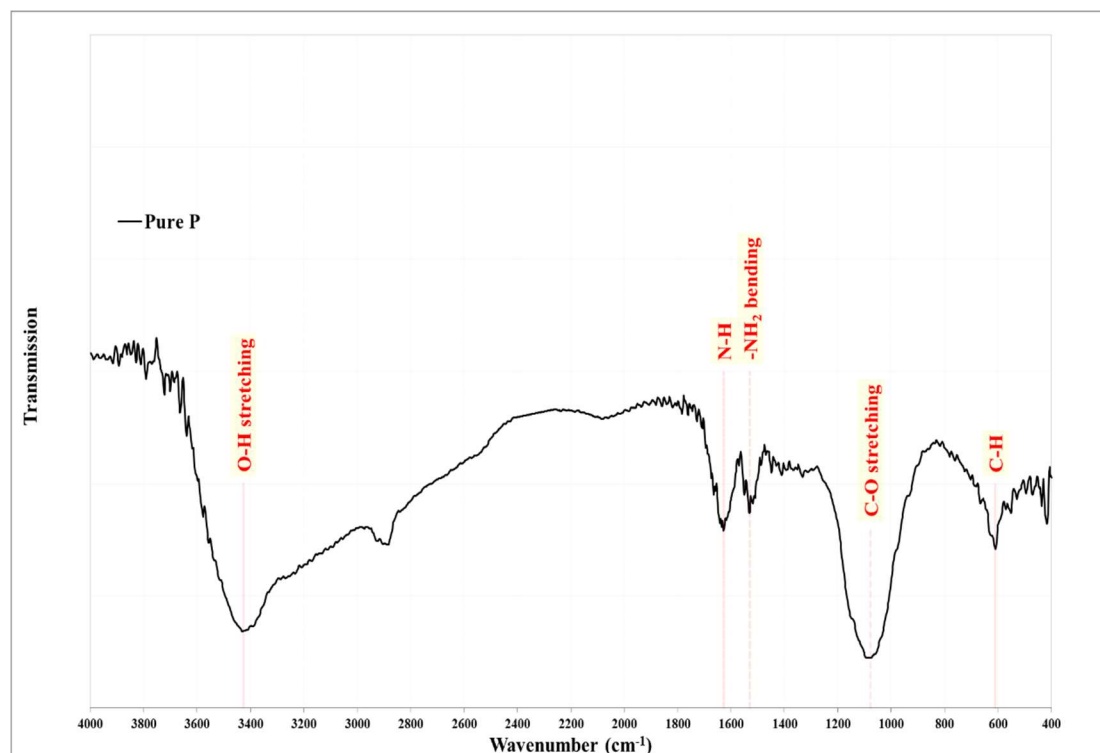


Figure 2 : FTIR spectrum of Paromomycin

The FTIR spectra of Chitosan, Paromomycin, and their composite nanoparticles at different ratios are presented in Figure (3). Notably, in the composite samples, the spectral bands exhibit shifts as the Paromomycin:chitosan ratio increases. Specifically, the band located at 1635.62 cm^{-1} for Amide I gradually decreases in energy, eventually reaching 1627.00 cm^{-1} for N-H vibration. Similarly, the -NH_2 bending vibration band shifts from 1539.22 to 1528.77 cm^{-1} , owing to the overlapping of these two bands originating from the two respective structures. Furthermore, as the ratio increases, certain bands diminish in intensity and eventually vanish. These bands are characteristic of the chitosan structure and include the Symmetric C-H deformation, Amide III, and Bridge O stretching vibrations, which are located at 1418.48 , 1322.40 , and 1158.26 cm^{-1} , respectively.

Conversely, other bands either evidence or become more pronounced with increasing the Paromomycin: chitosan ratio, corresponding to C-H vibrations at 2922.93 , 2885.02 , and 610.24 cm^{-1} .

All these variations in the FTIR spectra, including the appearance, weakening, or energy shifting of different absorption bands, reflect the success of the composite formation process and are indicative of the evolving composition ratio. These findings are consistent with prior research and studies in the field (Esfandiari *et al.*, 2019 and Andonegi, 2019). Table (1) lists the observed bands in all pure and composite samples.

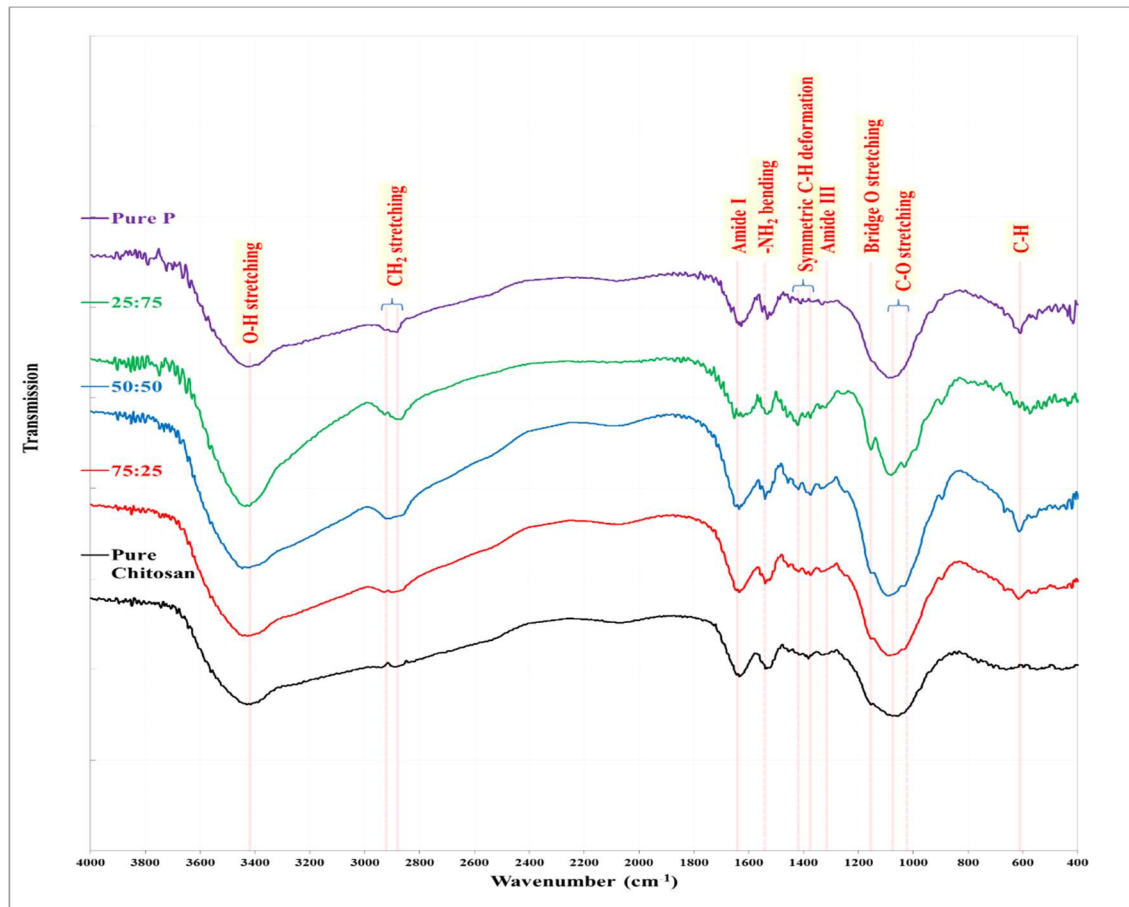


Figure *Error! No text of specified style in document.*: FTIR spectra of Chitosan, Paromomycin, and their composites nanoparticles

Table 1: FTIR bands list of Chitosan, Paromomycin, and their composites nanoparticles:

Band Type	Pure Chitosan	75:25	50:50	25:75	Pure P
O-H	3422.69	3424.41	3422.69	3427.86	3426.14
CH ₂	-	-	2916.04	2928.10	2922.93
	2871.30	2879.85	2866.06	2872.95	2885.02
Amide I	1635.62	1637.34	1639.06	1629.28	1627.00
-NH ₂ bending	1539.22	1538.11	1537.39	1530.12	1528.77
Symmetric C-H deformation	-	1418.48	1418.48	1420.20	-
	1375.39	1375.39	1375.39	1375.39	-
Amide III	1325.12	1322.40	-	1318.53	-
Bridge O stretching	-	1158.26	1153.09	1153.09	-
C-O stretching	1063.48	1085.88	1092.77	1082.43	1077.26

	-	-	-	1029.01	-
C-H	-	611.97	611.97	575.78	610.24

MTT assay

The assay of 3- (dimethylthiazol-2-yl)-2,5- diphenyltetrazolium bromide (MTT) stain was used to determine the cytotoxic effect of chitosan nano particles, paromomycin, and paromomycin conjugated nano chitosan on *E.histolytica* trophozoite. The MTT test for measuring cellular metabolic activity is widely used in investigations of cell toxicity; yet, it is frequently used and misinterpreted, this assay measures the viability of cells by measuring their reductive activity, which is the result of dehydrogenases in living cells' mitochondria converting the tetrazolium compound into water-insoluble formazan crystals. Reducing agents and enzymes from other organelles, such as the endoplasmic reticulum, are also involved (Ghasemi *et al.*, 2021).

The activity of *E.histolytica* trophozoite measured after (24) hours and possessing different concentrations (200, 100, 50, 25, 12.5) $\mu\text{g/mL}$ from nano chitosan and compared with paromomycin and paromomycin conjugated nano chitosan effect by measuring the activity of the trophozoite stage in different concentrations by using MTT assay. In each test there were three replicates and data are expressed as the mean \pm SD of three experiments.

Nano chitosan, paromomycin, and paromomycin conjugated nano chitosan demonstrated significant anti-parasitic activity against *E. histolytica* trophozoites *in vitro* at different concentrations. The activity of parasite trophozoites decreased with the increasing of nano chitosan concentration as when the concentrations were (200,100, 50, 25, 12.5) $\mu\text{g/mL}$ the activity was (56.87 ± 1.10 , 60.57 ± 1.39 , 74.88 ± 2.69 , 68.30 ± 2.22 and 95.06 ± 1.24) respectively (Table 2) ($P \geq 0.0001$) with IC_{50} s of $44.41 \mu\text{g/mL}$ after 24h.

Table (2): The activity of *E. histolytica* treated with chitosan nanoparticles by MTT assay after 24 hr.

Concentration $\mu\text{g/mL}$	200	100	50	25	12.5
Number of values	3	3	3	3	3
Mean	d 56.87	d 60.57	c 74.88	b 86.30	a 95.06
Std. Deviation	1.10	1.39	2.69	2.22	1.24
Std. Error of Mean	0.6351	0.8026	1.554	1.284	0.7146
(P ≥ 0.0001)					
means that do not share letters are significantly different					

For paromomycin, the trophozoite activity was (71.95 ± 0.096 , 83.26 ± 1.86 , 92.82 ± 1.01 , 94.95 ± 1.13 , and 94.83 ± 0.097) in concentrations (200, 100, 50, 25, 12.5) $\mu\text{g/mL}$ respectively ($P \geq 0.0001$) with IC_{50} s of $106.5 \mu\text{g/mL}$ after 24h. (Table 3).

Table (3): The activity of *E.histolytica* trophozoites treated with paromomycin drug by MTT assay after 24 hr

Concentration $\mu\text{g/mL}$	200	100	50	25	12.5
Number of values	3	3	3	3	3

Mean	c 71.95	b 83.26	a 92.82	a 94.95	a 94.83
Std. Deviation	0.96	1.86	1.01	1.13	0.97
Std. Error of Mean	0.5561	1.074	0.5825	0.6493	0.5603
(P ≥ 0.0001) means that do not share letters are significantly different					

The activity of *E.histolytica* trophozoite when treated with paromomycin conjugating nano chitosan (200, 100, 50, 25, 12.5) µg/mL was (50.13± 7.71, 57.97± 4.61, 71.37± 3.65, 82.35± 4.18 and 95.80± 2.68) respectively (Table 4.) (P ≥ 0.0001) with IC₅₀s of 27.47 µg/mL after 24h.

Table (4): The activity of *E.histolytica* trophozoites treated with paromomycin conjugating Nano chitosan by MTT assay after 24 hr

Concentration µg/mL	200	100	50	25	12.5
Number of values	3	3	3	3	3
Mean	d 50.13	d 57.97	c 71.37	b 82.35	a 95.80
Std. Deviation	7.71	4.61	3.65	4.18	2.68
Std. Error of Mean	4.448	2.659	2.109	2.415	1.549
(P ≥ 0.0001) means that do not share letters are significantly different					

Results listed in Table (2), (3) and (4) indicated an *in vitro* antiparasitic activity of CsNPs against *E. histolytica* trophozoites which in the same line with a study investigated the *in vitro* activity of chitosan and several of its derivatives and showed activity of chitosan against both extracellular promastigotes and intracellular amastigotes of *Leishmania major* and *Leishmania mexicana* (Riezk *et al.*, 2020).

Salem *et al.*, (2022) in an *in vivo* and *in vitro* study demonstrated Chitosan nanoparticle's potent nematocidal activity and are recommended to control *A. columba* infestation in pigeons.

The results also indicate that the lethal effect of nanochitosan on trophozoites increases with increasing concentration, and this is consistent with Elmi *et al.*, (2021) who indicated that treated trophozoites of *Trichomonas gallinae* showed more susceptibility to the highest concentration reaching mortality rate of 100% at 3h post-inoculation.

In the current study, paromomycin activity was elevated after conjugated with nanoparticles and this may be due to that hydrophilic and lipophilic chemotherapeutics combined with nanoparticles leading to an increase in the pharmacokinetic profile and therapeutic efficacy of the drugs via controlled release rates and site-specific delivery, thereby significantly lowering the side effects (Ghosh and Das *et al.*, 2023).

One important factor in nontoxicity is oxidative stress, it is known that a variety of nanoparticles can cause oxidative stress by producing reactive oxygen species (ROS) inside of cells, furthermore, interactions between nanoparticles and cells that because mitochondrial dysfunction might result in the formation of ROS. *In vivo*, nanoparticles trigger cytokine production, which releases free

radicals and reactive oxygen species (ROS) that cause secondary oxidative stress (Horie & Tabei, 2021).

Many studies have explained the high potential destructive activity of chitosan nanoparticles due to their ability to produce ROS. Jiang *et al.* (2019) found that CS NPs induced the massive generation of ROS with apoptotic activity against living cells. Also, a study done by Sarangapani *et al.* (2018) showed that the cellular uptake of chitosan nanoparticles was increased in a time-dependent manner and that the leukemia cells' ability to proliferate was inhibited in a dose-dependent manner with an elevation in reactive oxygen species (ROS) that was linked to an increased effect on apoptosis and caspase activity. The chitosan nanoparticles' increased capacity to scavenge free radicals reinforces their antioxidant properties.

Choi and Hu (2008) consider the reason for Chitosan nano particles anti parasitic activity is the interaction of NPs with the surface of parasites and it may be posited that NPs impair the structure of lipophosphoglycan and glycoprotein molecules that are found on the surface of parasites and which are responsible for the infection. They also proposed that these molecules may be more seriously affected from ROS generated from NPs and this may lead to inhibition of parasite infection.

1. Afzal, I., Sarwar, H. S., Sohail, M. F., Varikuti, S., Jahan, S., Akhtar, S., ... & Shahnaz, G. (2019). Mannosylated thiolated paromomycin-loaded PLGA nanoparticles for the oral therapy of visceral leishmaniasis. *Nanomedicine*, 14(4), 387-406.
2. Ali, E. N., Mohammed, S. T., Ajah, H. A., & Jamal, R. (2009). Preparation a New SHE-Medium Replacement of RPMI1640-Medium using Oral Rehydration Solution.
3. Andonegi, M., Las Heras, K., Santos-Vizcaíno, E., Igartua, M., Hernandez, R. M., de la Caba, K., & Guerrero, P. (2020). Structure-properties relationship of chitosan/collagen films with potential for biomedical applications. *Carbohydrate polymers*, 237, 116159.
4. Azad, Abul & Singh, Rohit & Sinha, Rani & Sinha, Keshav & Kumar, Munish. (2023). Metronidazole induced neurotoxicity: a case report. *International Journal of Basic & Clinical Pharmacology*. 12. 594-596. <https://doi.org/10.18203/2319-2003.ijbcp20231897>
5. Choi, O., & Hu, Z. (2008). Size dependent and reactive oxygen species related nanosilver toxicity to nitrifying bacteria. *Environmental science & technology*, 42(12), 4583-4588.
6. Ehrenkaufer, G. M., Haque, R., Hackney, J. A., Eichinger, D. J., & Singh, U. (2007). Identification of developmentally regulated genes in *Entamoeba histolytica*: insights into mechanisms of stage conversion in a protozoan parasite. *Cellular microbiology*, 9(6), 1426-1444.
7. El-araby, A., El Ghadraoui, L., & Errachidi, F. (2022). Usage of biological chitosan against the contamination of post-harvest treatment of strawberries by aspergillus niger. *Frontiers in Sustainable Food Systems*, 6, 881434.
8. Elmi, T., Rahimi Esboei, B., Sadeghi, F., Zamani, Z., Didehdar, M., Fakhar, M., ... & Tabatabaie, F. (2021). In vitro antiprotozoal effects of nano-chitosan on Plasmodium falciparum, Giardia lamblia and Trichomonas vaginalis. *Acta Parasitologica*, 66, 39-52.

9. Esfandiari, F., Motazedian, M. H., Asgari, Q., Morowvat, M. H., Molaei, M., & Heli, H. (2019). Paromomycin-loaded mannosylated chitosan nanoparticles: Synthesis, characterization and targeted drug delivery against leishmaniasis. *Acta tropica*, 197, 105072.
10. Flores-Huerta, N., Martínez-Castillo, M., Guzmán-Téllez, P., Silva-Olivares, A., Rosales-Morgan, G., Pacheco-Yépez, J., ... & Shibayama, M. (2024). *Entamoeba*. In *Molecular Medical Microbiology* (pp. 3069-3089). Academic Press.
11. Ghasemi, M., Turnbull, T., Sebastian, S., & Kempson, I. (2021). The MTT assay: utility, limitations, pitfalls, and interpretation in bulk and single-cell analysis. *International journal of molecular sciences*, 22(23), 12827.
12. Ghosh, S., Kar, N., & Das, M. (2023). Nanoparticle-based approach toward leishmaniasis treatment. In *Viral, Parasitic, Bacterial, and Fungal Infections* (pp. 449-465). Academic Press.
13. Gupta, P., Neupane, Y. R., Parvez, S., Kohli, K., & Sultana, Y. (2024). Combinatorial chemosensitive nanomedicine approach for the treatment of breast cancer. *Current Molecular Medicine*.
14. Hamad, H. K. (2021, December). Evaluation of Paromomycin Loaded Chitosan Nanoparticles and Oxidative Stress Activities against *Entamoeba Histolytica*. In *Journal of Physics: Conference Series*, 2114 (1), 012085. DOI 10.1088/1742-6596/2114/1/012085
15. Haque, R., Mondal, D., Duggal, P., Kabir, M., Roy, S., Farr, B. M., ... & Petri Jr, W. A. (2006). *Entamoeba histolytica* infection in children and protection from subsequent amebiasis. *Infection and immunity*, 74(2), 904-909.
16. Hemphill, A., Müller, N., & Müller, J. (2019). Comparative pathobiology of the intestinal protozoan parasites *Giardia lamblia*, *Entamoeba histolytica*, and *Cryptosporidium parvum*. *Pathogens*, 8(3), 116.
17. Horie, M., & Tabei, Y. (2021). Role of oxidative stress in nanoparticles toxicity. *Free radical research*, 55(4), 331-342.
18. Houpt, E., Hung, C. & Petri, W. (2016). *Entamoeba histolytica* (amebiasis). *Infectious Disease and Antimicrobial Agents*.
19. Jassim, Z. S. S. (2014). Immunological and histological effects of *Lactobacillus acidophilus* on *Entamoeba histolytica* infection. A Thesis Submitted to the Council of the College of Science Mustansiriyah University In Partial Fulfillment of the Requirements for the Degree of Master of Science in Biology/Zoology.
20. Jiang, Y., Yu, X., Su, C., Zhao, L., & Shi, Y. (2019). Chitosan nanoparticles induced the antitumor effect in hepatocellular carcinoma cells by regulating ROS-mediated mitochondrial damage and endoplasmic reticulum stress. *Artificial Cells, Nanomedicine, and Biotechnology*, 47(1), 747-756.
21. Khan, W., & Kumar, N. (2011). Drug targeting to macrophages using paromomycin-loaded albumin microspheres for treatment of visceral leishmaniasis: an in vitro evaluation. *Journal of drug targeting*, 19(4), 239-250.
22. Lee, S., Hao, L. T., Park, J., Oh, D. X., & Hwang, D. S. (2023). Nanochitin and nanochitosan: Chitin nanostructure engineering with multiscale properties for biomedical and

environmental applications. *Advanced Materials*, 35(4), 2203325.
<https://doi.org/10.1002/adma.202203325>

23. Riezk, A., Raynes, J. G., Yardley, V., Murdan, S., & Croft, S. L. (2020). Activity of chitosan and its derivatives against *Leishmania major* and *Leishmania mexicana* in vitro. *Antimicrobial agents and chemotherapy*, 64(3), 10-1128.

24. Rodrigues, C., de Mello, J. M. M., Dalcanton, F., Macuvele, D. L. P., Padoin, N., Fiori, M. A., ... & Riella, H. G. (2020). Mechanical, thermal and antimicrobial properties of chitosan-based-nanocomposite with potential applications for food packaging. *Journal of Polymers and the Environment*, 28, 1216-1236.

25. Salem, H. M., Salaeh, N. M., Ragni, M., Swelum, A. A., Alqhtani, A. H., Abd El-Hack, M. E., ... & Attia, M. M. (2022). Incidence of gastrointestinal parasites in pigeons with an assessment of the nematocidal activity of chitosan nanoparticles against *Ascaridia columbae*. *Poultry Science*, 101(6), 101820.

26. Sarangapani, S., Patil, A., Ngeow, Y. K., Elsa Mohan, R., Asundi, A., & Lang, M. J. (2018). Chitosan nanoparticles' functionality as redox active drugs through cytotoxicity, radical scavenging and cellular behaviour. *Integrative biology*, 10(5), 313-324.

27. Sivakami, M. S., Gomathi, T., Venkatesan, J., Jeong, H. S., Kim, S. K., & Sudha, P. N. (2013). Preparation and characterization of nano chitosan for treatment wastewater. *International Journal of Biological Macromolecules*, 57, 204-212.
<https://doi.org/10.1016/j.ijbiomac.2013.03.005>

28. Van Meerloo, J., Kaspers, G. J., & Cloos, J. (2011). Cell sensitivity assays: the MTT assay. *Cancer cell culture: methods and protocols*, 237-245.

29. Varma, R., & Vasudevan, S. (2020). Extraction, characterization, and antimicrobial activity of chitosan from horse mussel *modiolus modiolus*. *ACS omega*, 5(32), 20224-20230.

30. Zahra'a, A. A., Mustafa, T. A., Ardalan, N. M. & Idan, E. M. (2017). In vitro toxicity evaluation of silver nanoparticles on *Entamoeba histolytica* trophozoite. *Baghdad Science Journal*, 14(3), 509-515.